Supporting Information: Towards Custom Built Double Core Carbon Nanothreads by Stilbene and Pseudo-Stilbene Type Systems

Sebastiano Romi,[†] Samuele Fanetti,[*,‡,†] Frederico Alabarse,[¶] Antonio M. Mio,[§] Julien Haines,[‖] and Roberto Bini[*,†,⊥,‡]

†*European Laboratory for Nonlinear Spectroscopy (LENS), via Nello Carrara 1, 50019 Sesto Fiorentino (FI), Italy*

‡*Consiglio Nazionale delle Ricerche - Istituto di Chimica dei Composti OrganoMetallici, Via Madonna del Piano 10, 50019 Sesto Fiorentino (FI), Italy*

¶*Elettra Sincrotrone Trieste S.C.p.A, in AREA Science Park 34149 Basovizza, (TS), Italy*

§*IMM-CNR, Istituto per la Microelettronica e Microsistemi, VIII Strada 5 - Zona Industriale 95121 Catania, Italy*

‖*Institut Charles Gerhardt Montpellier, CNRS, Université de Montpellier - 34095 Montpellier, France*

⊥*Dipartimento di Chimica "Ugo Schiff", Università di Firenze, via della Lastruccia 3, 50019 Sesto Fiorentino (FI), Italy*

E-mail: fanetti@lens.unifi.it; roberto.bini@unifi.it

S1 - IR spectra

In Figure S1 we report the IR absorption spectra measured on decompression after the reaction completion of a pure TS sample at 31 GPa. In spite of releasing all the gas pressure from the membrane, the pressure inside the cell did not lower below 10 GPa and the cell should be manually opened.

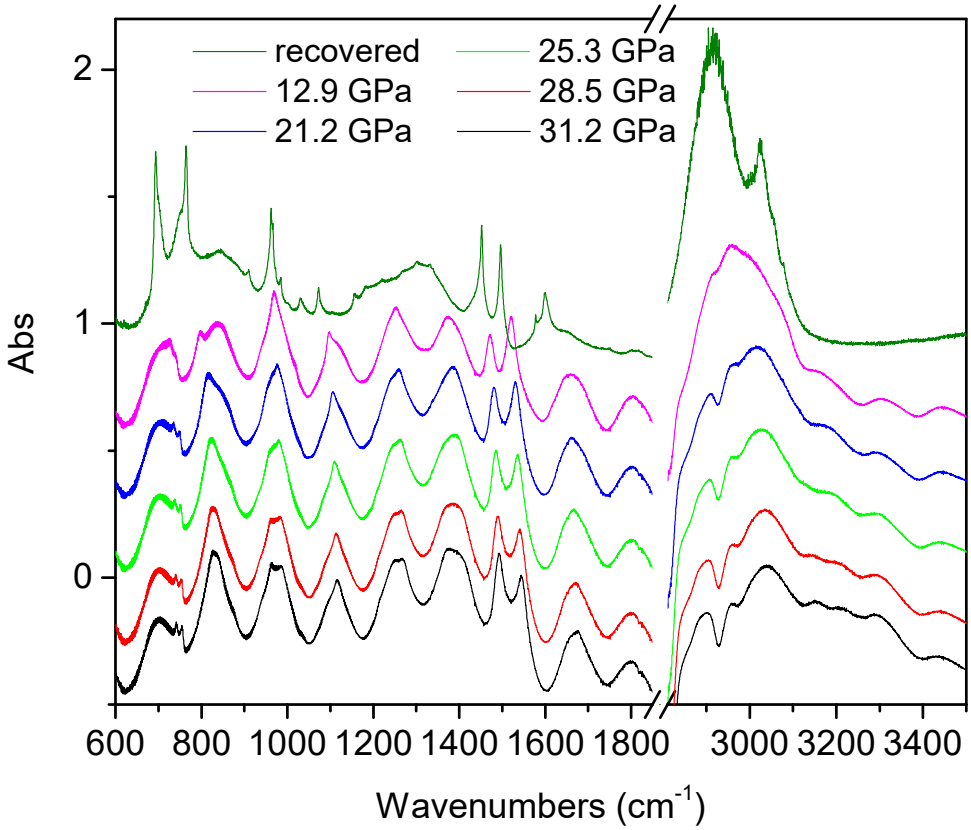

Figure S1: FTIR spectra measured during pressure release after the reaction was completed at 31 GPa.

In Figure S2 we report the comparison among selected IR absorption spectral windows of finely grounded pure TS, TA and 3(TS):1(TA) mixed crystal prepared according to the procedure described in the Methods section. The three spectra have been acquired at ambient temperature and at almost identical pressure values (1.6 GPa). The spectra have been overlapped in order to better judge relative intensity and position of the absorption bands.

As it can be seen the differences among the three spectra are rather evident allowing to exclude the formation of TA domains within TS crystals.

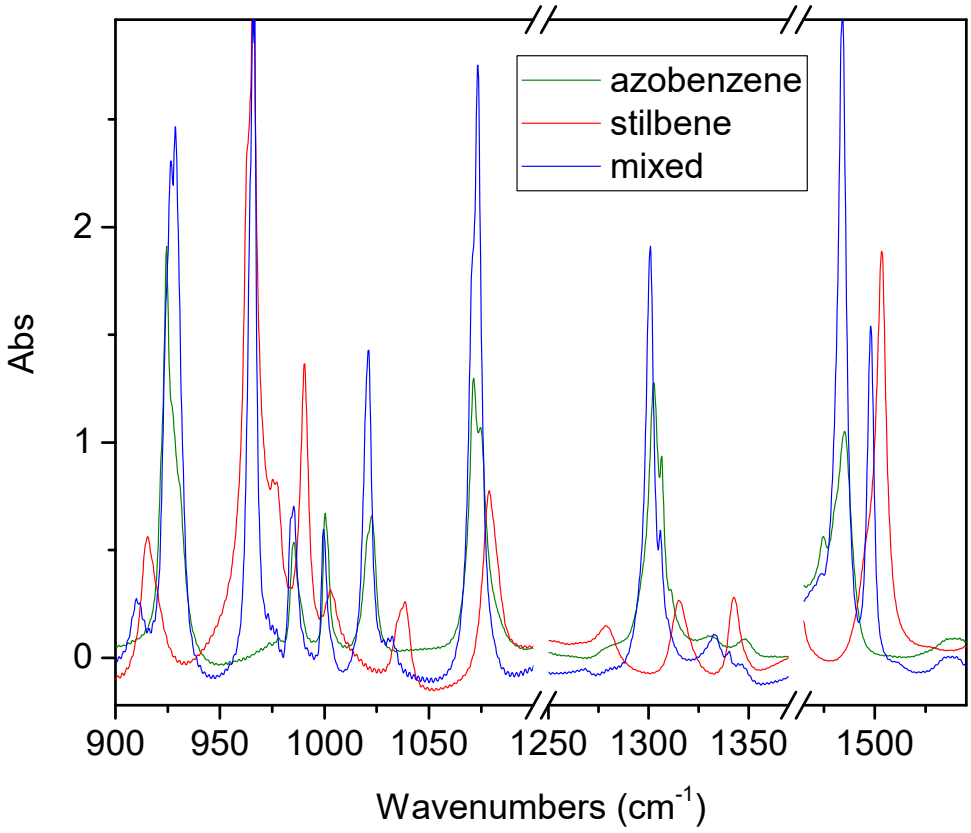

Figure S2: Comparison of selected portions of the IR spectra of TA, TS and 3(TS):1(TA) mixed crystal.

In Figure S3 we show selected IR absorption spectra of TS-TA mixed crystals collected during a room temperature compression up to the reaction threshold pressure whereas in Figure S4 we report the spectra measured at the beginning and at the end of the isobaric (8.8 GPa) heating of the TS-TA mixed crystal compressed up to 24.1 GPa.

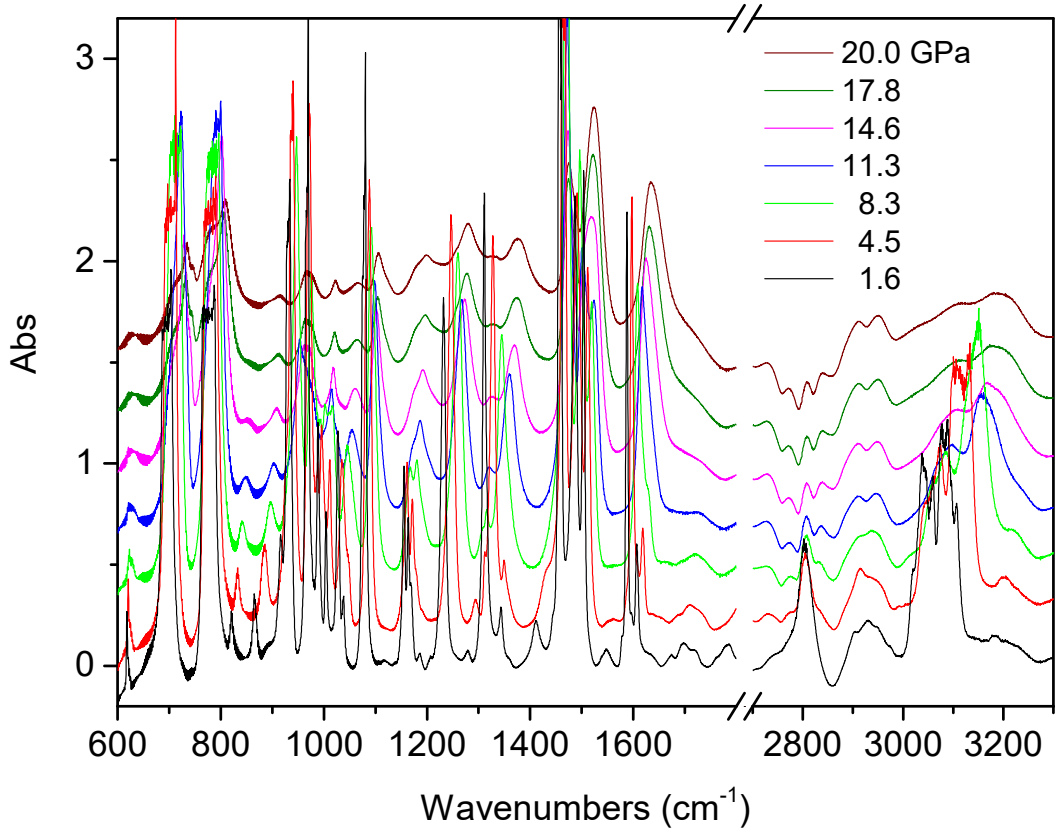

Figure S3: Pressure evolution of the IR spectra collected at ambient temperature on TS-TA mixed crystals.

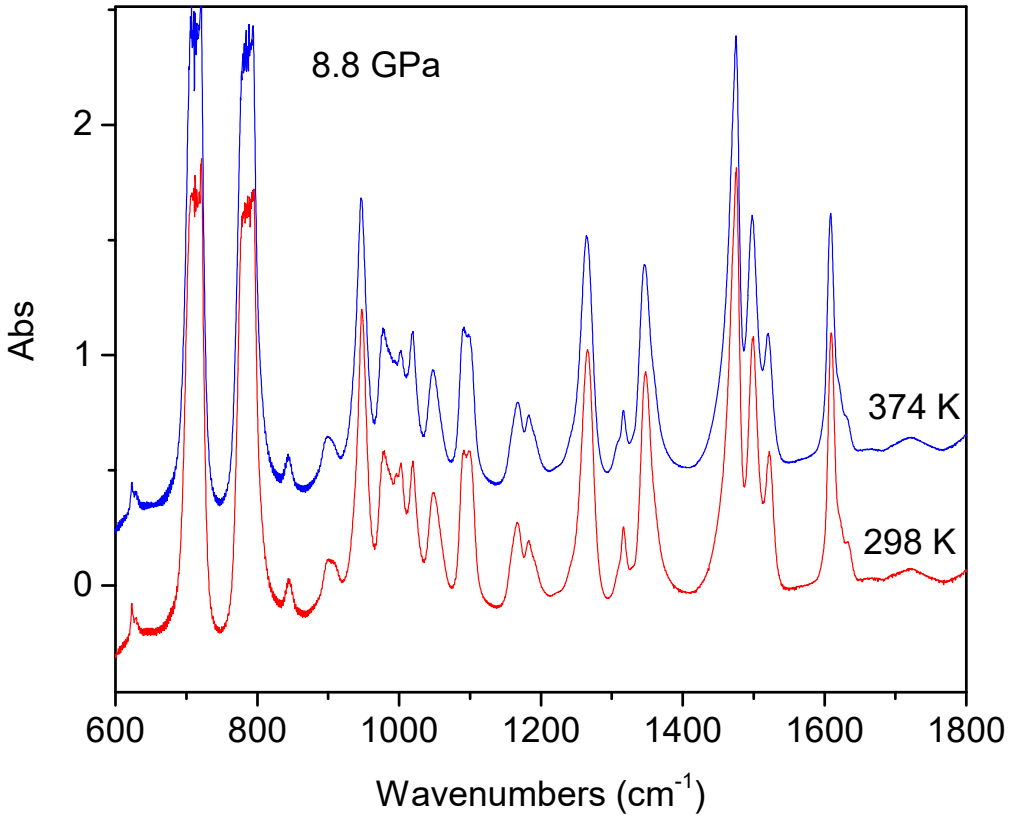

Figure S4: IR spectra collected at 8.8 GPa on TS-TA mixed crystals at ambient temperature and at about 100 °C temperature where the sample was compresed up to 24.1 GPa to study the reaction kinetics.

S2 - XRD

The patterns of the starting powders could be successfully and completely indexed up to about 7-8 GPa using the monoclinic $P2_1/c$ structure proper of both TS[S1,S2] and TS-TA mixed crystal.[S3] An example of Le Bail fit is reported in Figure S5 for a diffraction pattern measured on a TS-TA 1:1 mixed crystal after the cell closure (indexing and derived lattice parameters are reported in Table S1).

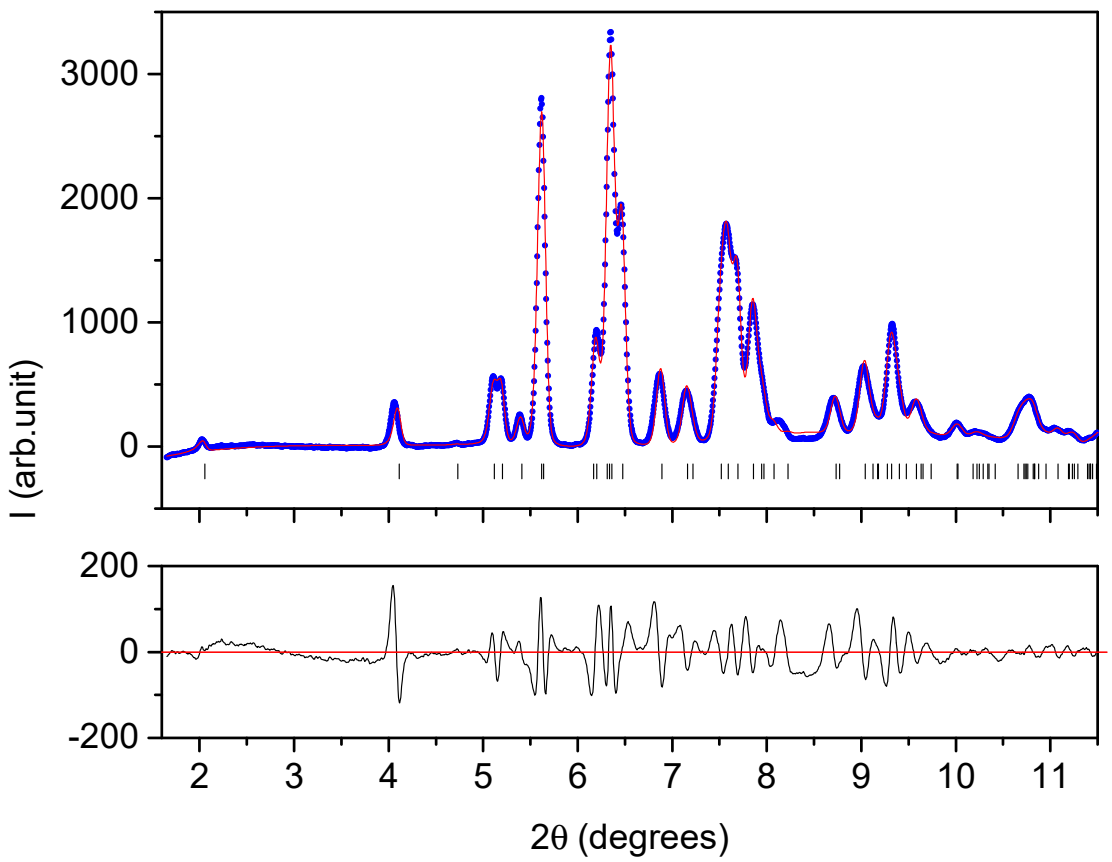

Figure S5: LeBail fit using the $P2_1/c$ structure to the synchrotron X-ray powder diffraction data (λ = 0.49499 Å) for polycrystalline TS-TA 1:1 mixed crystal measured at ambient temperature immediately after loading the cell. Blue points represent the experimental diffraction pattern, the red line represents the refined fit to the pattern, the black ticks mark (values and indexing reported in Table I) are the expected peak positions, while the black line on the bottom panel represents the difference curve.

As discussed in the manuscript a Rietveld refinement is prevented above 6 GPa by the powder

quality, strong preferred orientation and non-hydrostatic stress. In addition, above 9-10 GPa the sample is likely composed by a mixture of phases with overlapping peaks thus making the pattern indexing really challenging. Nevertheless, we could index all the diffraction peaks using a monoclinic structure. An example of the results is reported for TS in Table S2.

In Figure S6 the comparison between the diffraction patterns measured before and after the annealing procedure is reported. No significant changes are observed in the lineshape of the different peaks indicating that any substantial improvement of the nanothreads characteristics and of the lattice quality can be ruled out. However, a quite relevant increase of the d spacings (0.2-0.3 Å) is detected which could be related to the relaxation of the residual stress in the sample. The diffraction pattern of the annealed product is well reproduced by the same 2D monoclinic structure employed for TA with lattice parameters $a = 6.78$ Å; $c = 12.97$ Å; $\beta = 120°$ in perfect agreement with those observed in TA $a = 6.46$ Å; $c = 13.05$ Å; $\beta = 120°$.[S4]

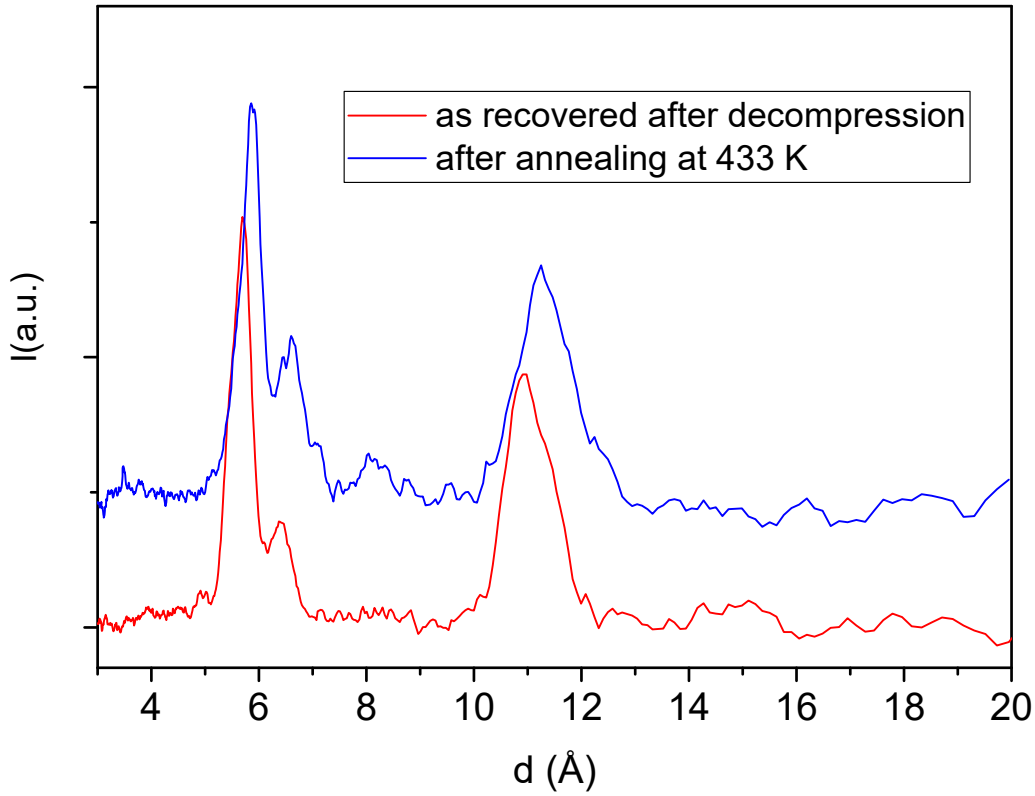

Figure S6: Comparison of 1D azimuthally integrated diffraction patterns as a function of the d spacing measured at ambient conditions on the sample recovered from the reaction performed in pure TS at 23.4 GPa and 373 K before and after a 1 hour thermal annealing performed at 433 K.

Table S1: Indexing relative to the X-ray diffraction pattern reported in Figure S5 according to the $P2_1/c$ structure. The resulting lattice parameters and the relative esd are $a = 14.897(3)$ Å, $b = 5.660(1)$ Å, $c = 11.965(3)$ Å, $\beta = 112.397(6)°$.

peak number	hkl	d (Å)	2θ(deg)	peak number	hkl	d (Å)	2θ(deg)
1	1 0 0	13.80268	2.05821	47	1 2 -1	2.74405	10.36645
2	2 0 0	6.90134	4.11708	48	4 0 -4	2.72691	10.43179
3	1 0 -2	5.99324	4.74123	49	3 1 2	2.665	10.67481
4	0 0 2	5.542	5.12752	50	2 1 -4	2.64942	10.73777
5	2 0 -2	5.45381	5.21049	51	1 2 1	2.64653	10.74952
6	1 1 0	5.24509	5.41799	52	4 1 1	2.64297	10.76403
7	0 1 1	5.0482	5.62947	53	2 2 -1	2.63918	10.77954
8	1 1 -1	5.03121	5.64849	54	5 1 -2	2.6257	10.83504
9	3 0 0	4.60089	6.17728	55	2 2 0	2.62255	10.84813
10	1 0 2	4.5751	6.21214	56	5 1 -1	2.6212	10.85371
11	1 1 1	4.49592	6.32166	57	1 1 -4	2.61132	10.89491
12	3 0 -2	4.47672	6.3488	58	3 1 -4	2.59262	10.97373
13	2 1 -1	4.46018	6.37237	59	1 2 -2	2.56291	11.10132
14	2 1 0	4.38125	6.48729	60	2 1 3	2.53792	11.211
15	1 1 -2	4.11901	6.90079	61	1 0 4	2.53658	11.21692
16	0 1 2	3.96342	7.17203	62	4 0 2	2.52852	11.2528
17	2 1 -2	3.93079	7.23165	63	0 2 2	2.5241	11.27258
18	2 1 1	3.77418	7.53215	64	2 2 -2	2.51561	11.31075
19	3 1 -1	3.73901	7.6031	65	5 1 -3	2.49356	11.41108
20	2 0 2	3.68883	7.70668	66	0 1 4	2.48964	11.42914
21	4 0 -2	3.61142	7.87213	67	6 0 -2	2.48669	11.44274
22	3 1 0	3.57278	7.95742	68	5 0 -4	2.48616	11.44518
23	1 1 2	3.56066	7.98455	69	5 1 0	2.48204	11.46424
24	3 1 -2	3.51369	8.09146	70	2 2 1	2.47307	11.50595
25	4 0 0	3.45067	8.23948	71	3 2 -1	2.4631	11.5527
26	1 1 -3	3.25033	8.7483	72	4 1 -4	2.45751	11.57906
27	2 1 -3	3.23675	8.78508	73	3 2 0	2.41373	11.7898
28	3 1 1	3.13989	9.05664	74	1 2 2	2.40998	11.8082
29	4 1 -1	3.11153	9.13937	75	3 2 -2	2.39526	11.88103
30	0 1 3	3.09556	9.18662	76	1 1 4	2.31547	12.29201
31	2 1 2	3.09212	9.19684	77	4 1 2	2.30933	12.3248
32	3 1 -3	3.06073	9.29137	78	1 2 -3	2.3066	12.33947
33	4 1 -2	3.0461	9.3361	79	2 2 -3	2.30173	12.36568
34	3 0 2	3.01922	9.4194	80	6 0 0	2.30045	12.3726
35	2 0 -4	2.99662	9.4906	81	2 0 4	2.28755	12.44264
36	5 0 -2	2.96244	9.60037	82	6 1 -2	2.27733	12.49869
37	4 1 0	2.94777	9.64825	83	5 1 -4	2.27692	12.50092
38	1 0 -4	2.94182	9.66781	84	3 2 1	2.26611	12.5608
39	3 0 -4	2.91516	9.75643	85	5 1 1	2.26234	12.58184
40	0 2 0	2.83523	10.03218	86	3 1 3	2.25618	12.61633
41	1 1 3	2.83345	10.0385	87	4 2 -1	2.25538	12.62081
42	4 1 -3	2.78924	10.19805	88	0 2 3	2.24928	12.6552
43	1 2 0	2.77725	10.2422	89	2 2 2	2.24796	12.66265
44	0 0 4	2.771	10.26534	90	6 1 -1	2.24563	12.67585
45	5 0 0	2.76054	10.30436	91	6 0 -4	2.23836	12.71719
46	0 2 1	2.74679	10.35606				

Table S2: Indexing of the reflections measured at 13.0 GPa compressing pure TS using a monoclinic unit cell (symmetry lower than $P2_1/c$). The resulting lattice parameters and the relative esd are $a = 13.25(3)$ Å, $b = 5.12(2)$ Å, $c = 11.47(3)$ Å, $\beta = 118.5(1)°$.

peak number	hkl	d (Å)	2θ(deg)
1	0 1 0	5.117	5.545
2	0 0 2	5.035	5.635
3	3 0 -2	4.183	6.784
4	1 1 -2	3.813	7.444
5	4 0 -2	3.292	8.623
6	3 1 0	3.097	9.168
7	4 0 0	2.906	9.770
8	4 1 -1	2.734	10.387
9	0 0 4	2.518	11.281

S3 - TEM

In Figure S7 we report representative TEM micrographs of amorphous regions collected on fragments of the sample recovered by the reaction of TS performed at 373 K and 23.3 GPa. Similar micrographs have also been obtained for other recovered materials from reactions involving TS and TS-TA mixed crystals.

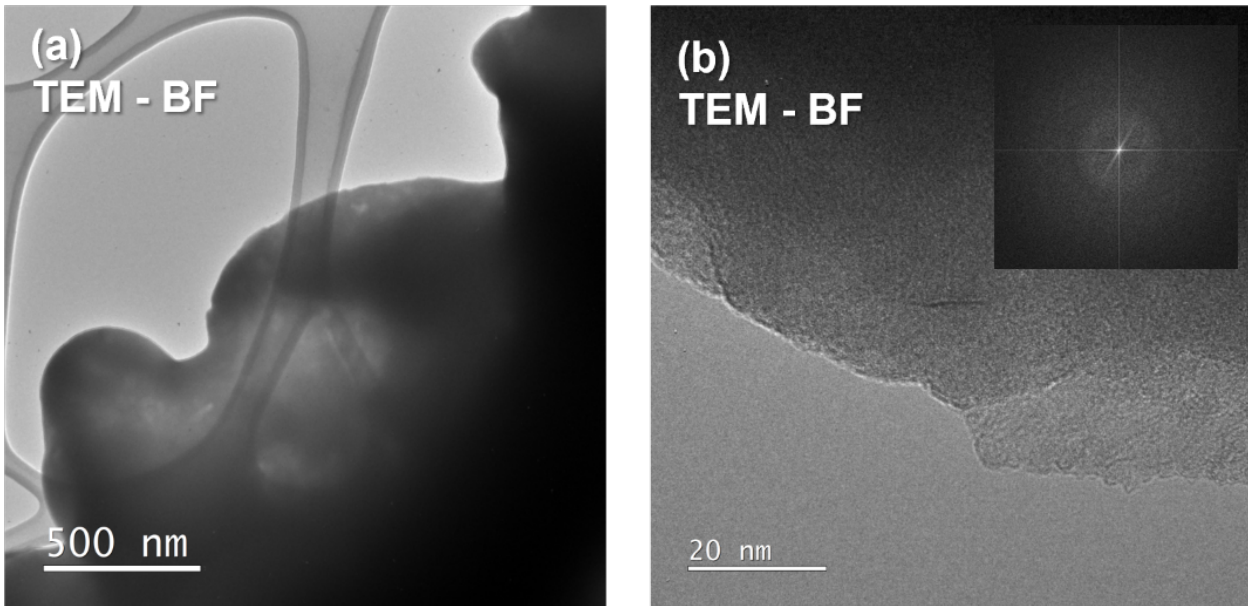

Figure S7: (a) Bright-field TEM micrograph acquired on the samples recovered at low magnification on the sample recovered by the reaction ù of TS performed at 373 K and 23.3 GPa. TEM analysis has been performed using an accelerating voltage of 60 kV, to avoid the knock-on damage. (b) Bright-field high-resolution TEM micrograph acquired on the border of (a), where the sample is thin enough for electron transmission. Amorphous phase is well visible, as also confirmed by the FFT in the inset.

S4 - DFT calculations

In Figure S8 we report the IR spectra computed for the oligomers made by six molecules having both the tube (3,0) and the polymer I structure. These spectra are compared with

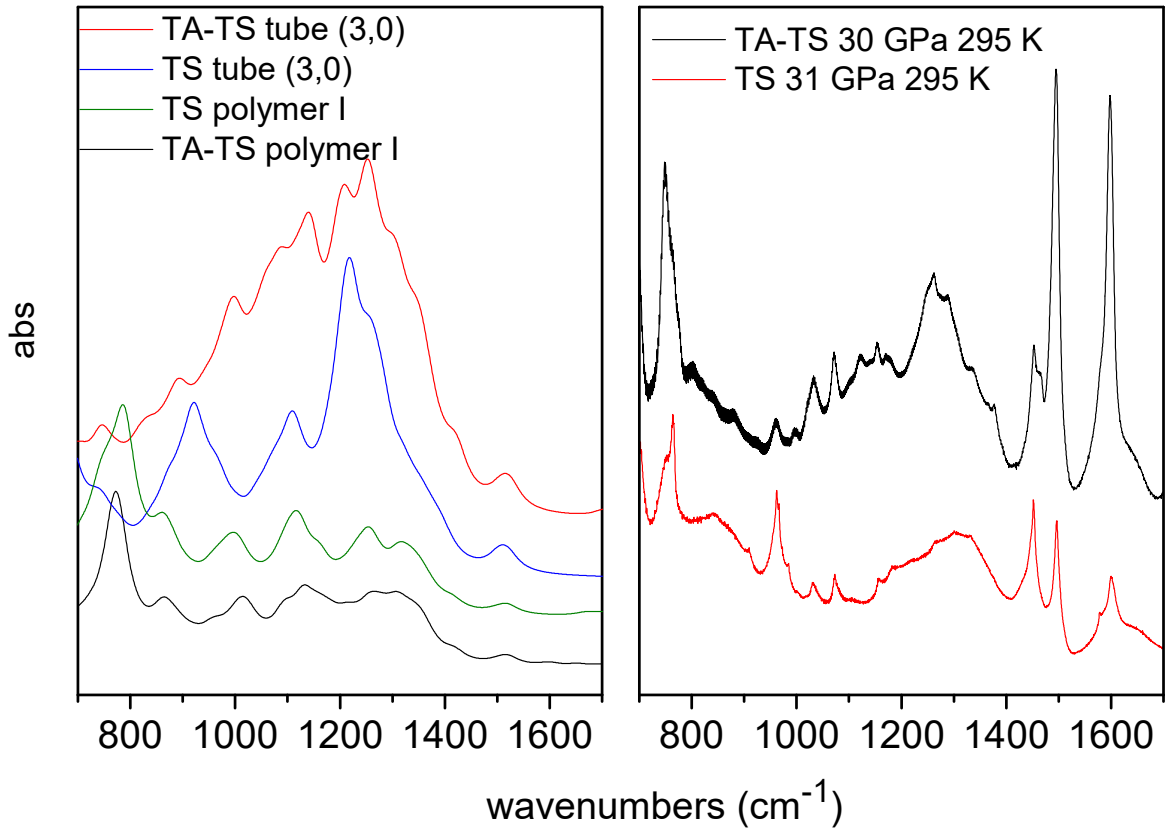

Figure S8: Comparison of the computed spectra (left panel) for the TS and TS-TA oligomers having both the tube(3,0) and polymer I geometry with those (right panel) of representative samples recovered from the ambient temperature reaction at 30 GPa.

those of two representative samples recovered from experiments performed around 30 GPa at ambient temperature. The computed spectra of the tube (3,0) oligomers which are characterized by the polymerization of the groups linking the nanothreads (Figure S9) present a remarkable intensification of the region between 1000 and 1400 cm^{-1} whereas the strong band around 800 cm^{-1} that dominates the spectra of the recovered materials is not observed. This band is assigned to bending modes involving the hydrogen atoms bound to the ethylenic

groups and it is indeed observed in the spectra computed for the polymer I structure which appears as the most probable structure for this nanothread. In Figure S10 we propose the

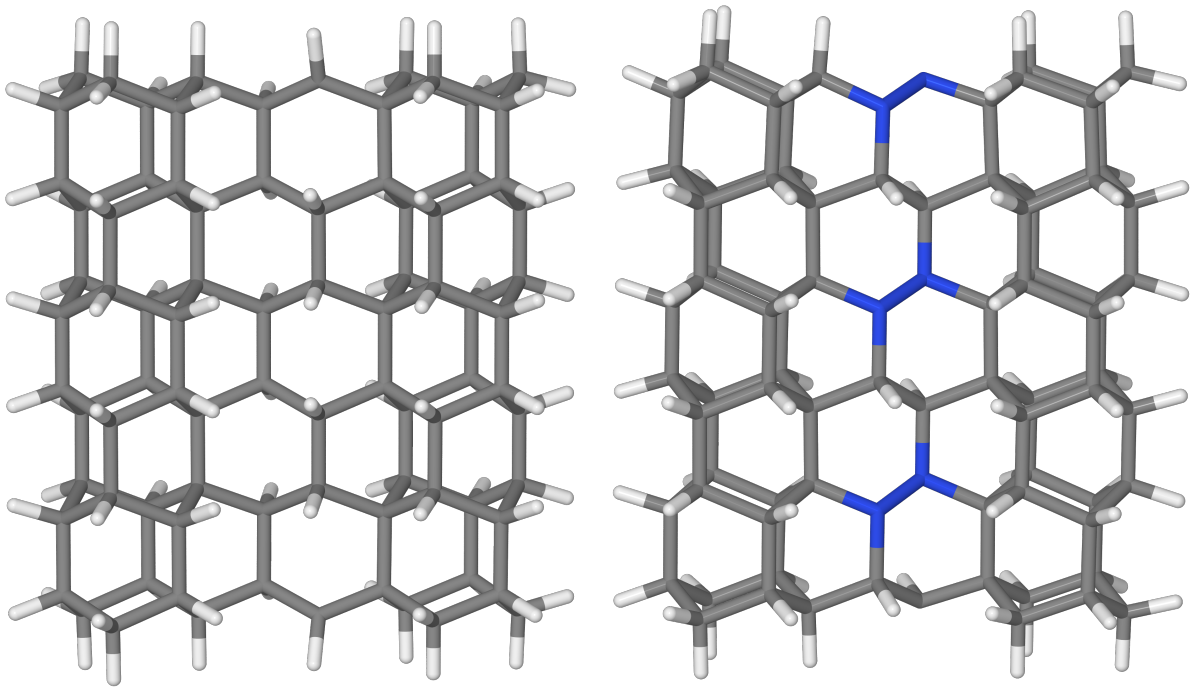

Figure S9: Computed structures for bot nanothreads from pure TS (left) and TS-TA (right) mixed crystals having the tube (3,0) structure. Polymerization along the axis thread of the linking ethylene and azo groups is observed.

reaction scheme leading to the polymer I thread. Para polymerization is followed by the zipping between closest rings involving adjacent not eclipsed positions (1-2', 1'-2, 5-4', 5'-4 using the nomenclature adopted by Chen et al.[S5]) as indicated by the dotted lines in the left picture. On the right the polymer I structure of the nanothread resulting from the reaction is shown.

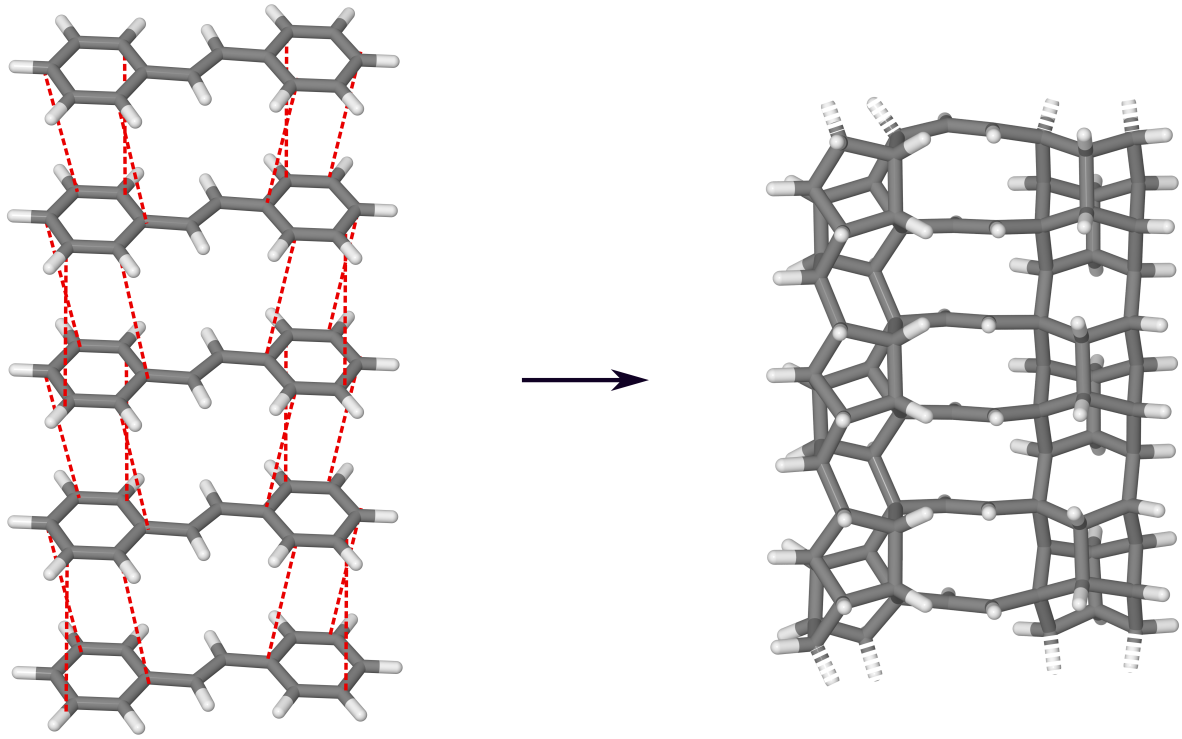

Figure S10: Polymer I structure (right panel) of the nanothread resulting from the compression of crystalline stilbene and indication (dotted lines) of the zipping direction through which the polymerization leading to the polymer I structure takes place.

References

(S1) J. A. Bouwstra, A. Schouten and J. Kroon, *J. Acta Crystallogr., Sect. C: Cryst. Struct. Commun.*, 1983, **C39**, 1121-1123.

(S2) J. A. Bouwstra, A. Schouten, J. Kroon and R. B. Helmholdt, *J. Acta Crystallogr., Sect. C: Cryst. Struct. Commun.*, 1984, **C40**, 428-431.

(S3) J. A. Bouwstra, A. Schouten, J. Kroon and R. B. Helmholdt, *J. Acta Crystallogr., Sect. C: Cryst. Struct. Commun.*, 1985, **C41**, 420-426.

(S4) S. Romi, S. Fanetti, F. Alabarse, A. M. Mio and R. Bini, *Chem. Sci.*, 2021, **12**, 7048-7057.

(S5) B. Chen, R. Hoffmann, N. W. Ashcroft, J. Badding, E. S. Xu and V. H. Crespi, *J. Am. Chem. Soc.*, 2015, **137**, 14373-14386